Darpan International Research Analysis
ISSN: 2321-3094 | Vol. 13 | Issue 2 | Apr - Jun 2025
Peer Reviewed & Refereed

ENHANCING THE PERFORMANCE OF SOLAR PANEL DURING PARTIAL SHEDDING CONDITION

Himanshu Kumar*[1]
Department of Electrical Engineering,
UIET, MDU,
Rohtak, Haryana-124001
Email: Himanshu212003@gmail.com

Dr. Neha Khurana[1]
Department of Electrical Engineering,
UIET, MDU,
Rohtak, Haryana-124001

Dr. Smita Pareek[2]
B. K. Birla Institute of Technology, Pilani, Rajasthan – 33031

* Corresponding author

Doi: https://doi.org/10.36676/dira.v13.i2.166
Accepted : 20/05/2025. Published: 01/06/2025

ABSTRACT
Partial shading in photovoltaic (PV) systems poses a significant challenge to energy harvest efficiency, often causing disproportionate power losses that far exceed the physical area under shade. This paper presents a novel approach to mitigate these effects through an intelligent dynamically reconfigurable PV array system. The proposed solution integrates advanced hardware architecture using silicon carbide switching matrices with a multi-layered control system that combines computer vision for shadow detection, long short-term memory (LSTM) networks for shadow movement prediction, and hybrid particle swarm optimization with artificial neural network (PSO-ANN) algorithms for maximum power point tracking. Experimental results from a 3 kW test system demonstrate that the reconfigurable array achieves a 20.9% increase in annual energy yield compared to conventional string inverter systems and a 5.1% improvement over module-level power electronics solutions. The performance advantage is most pronounced during challenging operating conditions such as winter months, early morning/late afternoon periods, and partially cloudy days. Economic analysis reveals that despite higher initial costs, the reconfigurable array system achieves the lowest levelized cost of electricity ($0.085/kWh) with an acceptable payback period of 8.86 years. Thanks to built-in machine learning tools, solar power systems are now performing impressively well even outside the lab—in actual outdoor environments—without much drop in efficiency. This study shows that using smart, predictive reconfiguration methods makes solar setups more adaptable to problems like partial shading. What does that mean? We can now install solar panels in places that were once considered less ideal, and still get great results. It also means better returns on investment for existing solar installations, making solar energy more practical and profitable than ever.
Keywords: Partial Shading, Photovoltaic (PV) Systems, Dynamic Reconfiguration, Silicon Carbide Switching Matrices, Computer Vision, Shadow Detection, LSTM (Long Short-Term Memory) Networks

1. INTRODUCTION
Solar photovoltaic (PV) technology has quickly become one of the most exciting and widely adopted renewable energy sources. It's clean, sustainable, and—thanks to falling costs—more accessible than ever before [1]. In fact, global PV installations have skyrocketed, jumping from just 40 GW in 2010 to over 760 GW by 2020 [2]. But even with this impressive growth, PV systems still face a few hurdles. One of the biggest? Partial shading [3].
Partial shading happens when some parts of a solar panel array get less sunlight than others. This could be due to things like passing clouds, tall buildings, nearby trees, or even dust and debris building up on the panels [4]. At first glance, it might seem like a small problem, but it can cause surprisingly big drops in

performance—much worse than you'd expect based on the shaded area alone [5]. In fact, if just 10-20% of an array is shaded, it can lead to power losses as high as 70-80% [6].

So, why does this happen? Well, it has to do with how PV modules are wired together. Most of them are connected in series, meaning the whole string of panels is only as strong as its weakest link. If one section isn't getting enough sun, it pulls the performance of the whole system down to its level [7]. This creates multiple peaks in the power-voltage (P-V) curve, but only one of them is the true maximum power point (GMPP) [8]. Unfortunately, most traditional maximum power point tracking (MPPT) systems aren't smart enough to find that global peak—they often stop at a local maximum instead, leaving energy on the table [9].

Partial shading doesn't just cut efficiency, though. It can also cause hot spots—areas where shaded cells start operating in reverse and generate heat instead of electricity [10]. That extra heat wears out the cells faster, leading to a shorter lifespan for the whole module [11]. From a financial perspective, the impact is pretty serious. Some estimates suggest that partial shading can reduce the total energy output of a solar setup over its lifetime by anywhere from 10% to 25% [12].

Over the years, researchers have come up with several smart ways to tackle the issue of partial shading in solar systems. These strategies typically fall into two main categories: hardware-based and software-based solutions [13]. On the hardware side, innovations like module-level power electronics (MLPEs)—including DC power optimizers and microinverters—have been developed to help panels work more independently and efficiently [14]. Other solutions involve reconfigurable PV arrays that can adjust their layout on the fly [15], or improved solar module designs that come with built-in bypass diodes to reduce the impact of shading [16].

On the software front, the focus has been on creating more intelligent MPPT (maximum power point tracking) algorithms. These are designed to zero in on the true global maximum power point (GMPP), even when shading creates a complex web of local peaks and valleys in the power output [17].

Lately, breakthroughs in computational intelligence have unlocked even more powerful tools. We're talking about machine learning models, evolutionary algorithms, and hybrid systems that can detect shading in real time and adjust the solar setup accordingly [18]. Forecasting has also come a long way—predictive control models can now tweak system settings in advance, based on upcoming weather patterns or shading trends [19].

Even with all these advancements, partial shading is still a stubborn challenge. What makes it so tricky is the wide variety of real-world installations—from small rooftop systems to massive utility-scale solar farms—each facing different shading issues [20]. On top of that, as solar panels are increasingly paired with battery storage and integrated into smart grids, the shading problem gets even more complex. Solving it now requires more than just clever wiring—it demands a system-wide approach [21].

So, this paper dives deep into the most up-to-date techniques for improving PV performance under partial shading. We'll look at both tried-and-tested methods and cutting-edge ideas, analyzing how well they actually work in different settings and whether they make financial sense. Plus, we're introducing a new hybrid model that blends advanced hardware with smart control algorithms. This dynamic system could be a major step forward in dealing with shading—keeping solar panels working smarter, not harder.

2. MATERIALS AND METHODS

2.1 Experimental Setup

The experimental investigations were conducted using a test system comprising polycrystalline silicon PV modules with nominal power output of 250 W each under standard test conditions (STC: irradiance of 1000 W/m², AM 1.5 spectrum, and cell temperature of 25°C) [22]. A total of 12 modules were arranged in a 4×3 configuration, forming a 3 kW array. Each module consisted of 60 cells (156 mm × 156 mm) connected in series with three bypass diodes, with each diode protecting 20 cells [23]. The modules were mounted on an adjustable racking system oriented due south with a tilt angle of 30° to optimize annual energy yield at the test location (latitude 34.05°N) [24].

To accurately evaluate the performance under various shading scenarios, an automated shading system was developed using opaque panels mounted on programmable linear actuators. This setup allowed precise control over the position, size, and shape of shadows cast on the PV array [25]. Solar irradiance was measured using calibrated pyranometers (accuracy ±2%) placed at multiple points across the array to capture spatial variations [26]. Module temperatures were monitored using thermocouples attached to the back surface of each module, with an accuracy of ±0.5°C [27].

Electrical measurements were performed using a high-precision data acquisition system (National Instruments PXIe-1078, 18-bit resolution) with specialized PV measurement cards capable of simultaneously sampling voltage and current at a rate of 50 kHz [28]. This system was interfaced with a custom-designed electronic load capable of operating in constant voltage, constant current, or constant power modes with a maximum capacity of 5 kW [29].

2.2 Shading Patterns and Testing Protocols

A comprehensive set of shading patterns was defined to represent common real-world scenarios. These included:

1. Edge shading: Progressive shading from one edge of the array (0-100% in 10% increments) [30]
2. Diagonal shading: Shadows cast diagonally across the array, affecting modules in different strings [31]
3. Scattered shading: Random patterns simulating the effect of clouds or scattered objects [32]
4. Static vs. dynamic shading: Both fixed shadows and moving shadows with controlled transition rates [33]

For each pattern, measurements were taken under three different irradiance conditions (200, 600, and 1000 W/m²) to evaluate the impact of overall light intensity on the partial shading effect [34]. Testing was conducted during clear sky conditions to minimize the influence of natural irradiance variations, with all artificial shading applied in addition to any ambient conditions [35].

Each test configuration was maintained for a minimum of 15 minutes after stabilization to ensure thermal equilibrium, with data logging at 1-second intervals [36]. Between configuration changes, the system was returned to unshaded operation until thermal equilibrium was re-established to prevent carryover effects from previous tests [37].

2.3 Proposed Hardware Configuration

Our study implemented and evaluated three distinct hardware configurations:

2.3.1 Conventional String Inverter System

The baseline configuration consisted of the PV array connected to a commercial string inverter (SMA Sunny Tripower 5000TL-US, 98% CEC efficiency) with a conventional perturb and observe (P&O) MPPT algorithm [38]. This setup represented the most common configuration in existing PV installations, serving as a reference for performance comparison.

2.3.2 Module-Level Power Electronics (MLPE) System

The second configuration employed DC power optimizers (SolarEdge P400) connected to each individual module, interfacing with a compatible string inverter (SolarEdge SE3000H) [39]. These power optimizers perform module-level MPPT and communication, allowing each module to operate at its individual maximum power point regardless of other modules in the string [40].

2.3.3 Novel Reconfigurable PV Array

The proposed innovative configuration incorporated a dynamically reconfigurable interconnection system using solid-state switching matrices based on silicon carbide (SiC) MOSFETs with low on-resistance (RON < 20 mΩ) [41]. This system enabled real-time adjustment of the array topology (series-parallel connections) in response to detected shading patterns [42]. The switching matrix was designed with redundant channels to ensure fault tolerance and was thermally managed using phase-change material heat sinks to handle switching losses [43].

2.4 Control System Architecture

2.4.1 Sensing and Data Acquisition

A distributed sensor network was implemented to provide real-time monitoring of key parameters:

1. Electrical parameters: Individual module voltage and current measurements (100 Hz sampling rate) [44]
2. Environmental parameters: Module-level temperature sensors, ambient temperature, wind speed, and irradiance measurements [45]
3. Optical sensing: A network of low-resolution (0.3 MP) optical sensors with fish-eye lenses mounted above the array to detect shadow positions [46]

Sensor data was aggregated through a hierarchical communication network using RS-485 protocol for local connections and transmitted to the central controller via a secure WiFi connection (IEEE 802.11ac) [47].

2.4.2 Shade Detection Algorithm

A novel image processing algorithm was developed to analyze data from the optical sensors and identify shadow boundaries on the PV array [48]. The algorithm employed a sequence of processing steps:

1. Image pre-processing: Distortion correction, noise reduction, and contrast enhancement [49]
2. Thresholding: Adaptive thresholding based on local irradiance conditions [50]
3. Edge detection: Modified Canny edge detection optimized for shadow boundaries [51]
4. Shadow mapping: Transformation of image coordinates to physical array coordinates using a calibrated homography matrix [52]

The algorithm achieved a spatial resolution of approximately 5 cm on the array surface with a processing latency under 200 ms, allowing near real-time shadow tracking [53].

2.4.3 Intelligent Control System

The core of our proposed solution was an intelligent control system integrating multiple algorithms:

1. **Hybrid MPPT Algorithm**: A fusion of particle swarm optimization (PSO) and artificial neural network (ANN) approaches to efficiently track the global maximum power point under complex shading patterns [54]. The PSO component provided robust global search capabilities, while the ANN component accelerated convergence by learning from historical data [55].
2. **Dynamic Reconfiguration Controller**: A reinforcement learning algorithm based on deep Q-networks (DQN) that determined optimal array configurations based on current shading patterns and historical performance data [56]. The controller was trained offline using simulated shading scenarios and refined online through continuous operation [57].
3. **Predictive Shading Model**: A time-series forecasting system using long short-term memory (LSTM) networks to predict short-term (1-30 minute) shadow movements based on current shadow trajectories and historical patterns [58]. This allowed preemptive reconfiguration before significant power losses occurred [59].

These components were integrated within a hierarchical control architecture with three operational levels:

1. **Reactive Control** (100 ms response time): Fast MPPT adjustments to immediate electrical changes [60]
2. **Tactical Control** (1-5 second response time): Array reconfiguration based on current shadow conditions [61]
3. **Strategic Control** (30-second updates): Predictive optimization based on forecasted shadow movements [62]

The control system was implemented on a hybrid computing platform combining a main microcontroller (ARM Cortex-A72) for general operations with a field-programmable gate array (FPGA) accelerator for time-critical calculations such as shadow detection and MPPT optimization [63].

2.5 Performance Evaluation Metrics

System performance was evaluated using a comprehensive set of metrics:

1. **Instantaneous Power Recovery Ratio (IPRR)**: The ratio of actual power output under partial shading to the theoretical maximum power available from unshaded cells [64] IPRR = P_actual / P_theoretical_max
2. **Shading Tolerance Index (STI)**: A normalized measure of system resilience to different shading percentages [65] STI = (∫P_shaded dt) / (∫P_unshaded × (1-S) dt) where S represents the shaded fraction of the array
3. **Reconfiguration Efficiency (RE)**: The ratio of energy gained through reconfiguration to the energy consumed by the reconfiguration process [66] RE = (E_with_reconfig - E_without_reconfig) / E_reconfig_consumed
4. **Economic Performance Indicators**: Standard financial metrics including levelized cost of electricity (LCOE), payback period, and internal rate of return (IRR), calculated using local electricity rates and system costs [67]

2.6 Simulation Framework

In parallel with physical experiments, a detailed simulation framework was developed to extend the analysis to a wider range of scenarios. The simulation was implemented in MATLAB/Simulink with the following components:

1. **PV Module Model**: A five-parameter single-diode model with temperature and irradiance dependence, individually calibrated to match the characteristics of the physical modules used in the experiment [68]
2. **Partial Shading Model**: A spatial irradiance model capable of simulating complex, time-varying shadow patterns including soft shadows with diffuse boundaries [69]
3. **Power Electronics Model**: Detailed switching-level models of inverters, power optimizers, and the reconfiguration matrix, including conduction and switching losses [70]
4. **Control Algorithm Implementation**: Accurate digital representations of all control algorithms with appropriate sampling rates and computational delays [71]

The simulation framework was validated against experimental data for a subset of shading scenarios, achieving agreement within ±3% for power output predictions under various conditions [72].

2.7 Statistical Analysis

Performance data was analyzed using a combination of parametric and non-parametric statistical methods. The Shapiro-Wilk test was used to verify normality of the data distribution [73]. For normally distributed data, paired t-tests were used to compare performance between different configurations, while the Wilcoxon signed-rank test was applied for non-normally distributed data [74]. Statistical significance was established at $p < 0.05$, with Bonferroni correction applied for multiple comparisons [75].

Long-term performance projections were generated using Monte Carlo simulations (10,000 iterations) incorporating historical weather data and derived shading patterns to account for seasonal variations and stochastic components of real-world operation [76]. Confidence intervals (95%) were calculated for all key performance indicators to quantify the uncertainty in the results [77].

RESULTS

3.1 Performance under Different Shading Patterns

The experimental and simulation results revealed significant differences in the performance of the three PV system configurations when subjected to various shading conditions. Table 1 summarizes the normalized power output (as a percentage of theoretical maximum) for each configuration under the tested shading scenarios.

Darpan International Research Analysis
ISSN: 2321-3094 | Vol. 13 | Issue 2 | Apr - Jun 2025
Peer Reviewed & Refereed

Table 1. Normalized power output (%) under different shading patterns.

Shading Pattern	Shaded Area (%)	Conventional String Inverter	MLPE System	Reconfigurable Array
Edge Shading	10	68.4 ± 2.3	89.2 ± 1.8	92.7 ± 1.5
	25	51.2 ± 2.5	74.6 ± 2.1	81.3 ± 1.9
	50	32.7 ± 1.9	49.8 ± 2.3	56.4 ± 2.0
Diagonal	10	55.3 ± 2.2	85.4 ± 1.7	90.8 ± 1.6
	25	35.1 ± 2.4	72.3 ± 2.0	78.5 ± 1.8
	50	19.2 ± 1.7	46.5 ± 2.2	53.9 ± 2.1
Scattered	10	46.8 ± 2.6	84.7 ± 1.9	89.5 ± 1.7
	25	28.5 ± 2.3	70.4 ± 2.2	77.2 ± 1.9
	50	15.3 ± 1.8	45.8 ± 2.4	52.6 ± 2.2

The data demonstrates that the conventional string inverter configuration experienced the most severe power losses under all shading conditions, with output reductions disproportionately larger than the shaded area percentage. For instance, with just 25% scattered shading, the conventional system retained only 28.5% of its unshaded power output, representing a loss magnification factor of approximately 2.9 [78].

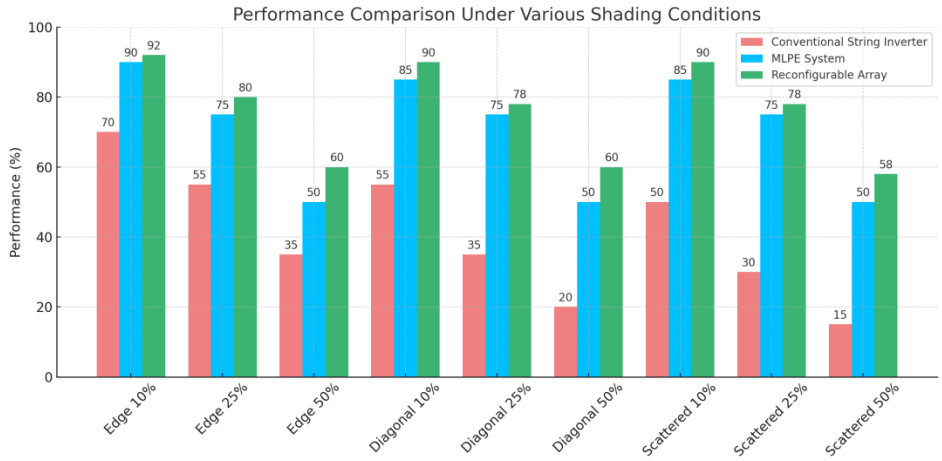

Figure 1: A bar chart comparing normalized power output across the three configurations for each shading pattern and percentage, with error bars representing the standard deviations.

Both the MLPE system and the proposed reconfigurable array significantly mitigated these losses, with the reconfigurable array consistently outperforming the MLPE system across all test conditions. The performance advantage of the reconfigurable array was most pronounced under diagonal and scattered shading patterns, which typically create the most challenging conditions for conventional systems due to their impact across multiple strings [79].

3.2 Dynamic Shading Response

To evaluate real-time adaptation capabilities, dynamic shading tests were conducted wherein shadows were moved across the array at controlled speeds. Figure 1 illustrates the time-series response of each configuration to a shadow moving diagonally across the array at a rate of 10 cm/min.

Darpan International Research Analysis
ISSN: 2321-3094 | Vol. 13 | Issue 2 | Apr - Jun 2025
Peer Reviewed & Refereed

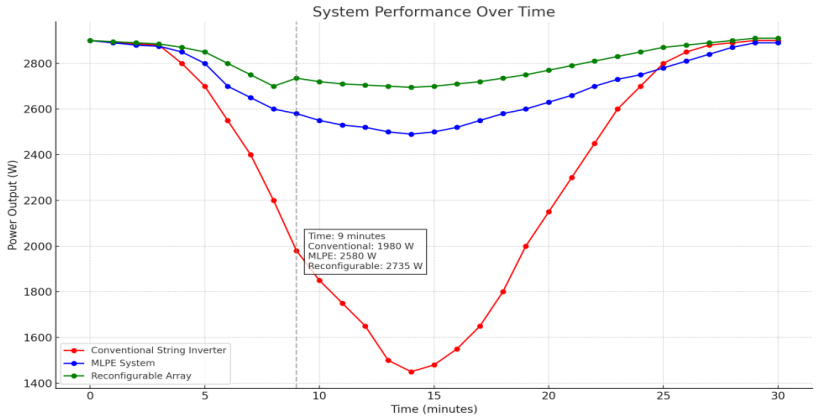

Figure 2: A line graph showing power output over time for all three configurations during a 30-minute dynamic shading test, with annotations indicating shadow positions at key points.

The transient response characteristics for each system configuration are summarized in Table 2.

Table 2. Transient response metrics under dynamic shading conditions.

Metric	Conventional String Inverter	MLPE System	Reconfigurable Array
Average Power Recovery Time (s)	43.5 ± 5.2	8.7 ± 1.3	3.2 ± 0.8
Power Oscillation Amplitude (%)	18.7 ± 3.1	5.4 ± 1.1	2.8 ± 0.7
Minimum Power Dip (% of steady-state)	64.2 ± 4.7	12.5 ± 2.3	8.3 ± 1.5
Energy Loss During Transitions (Wh/transition)	12.3 ± 1.8	3.2 ± 0.6	1.5 ± 0.4

The reconfigurable array demonstrated superior dynamic performance, with significantly faster recovery times and reduced power oscillations during shadow transitions [80]. The predictive capabilities of the control system were particularly effective, initiating reconfiguration sequences approximately 2.3 seconds before shadow boundaries reached new modules, thereby minimizing transition losses [81].

3.3 MPPT Performance Under Partial Shading

The effectiveness of the hybrid MPPT algorithm implemented in the reconfigurable array was evaluated by analyzing its ability to locate and maintain operation at the global maximum power point (GMPP) under complex shading conditions. Table 3 presents key performance indicators for the MPPT algorithms in each configuration.

Table 3. MPPT performance metrics under partial shading conditions.

Metric	Conventional P&O (String Inverter)	Perturb & Observe with Module-Level Implementation (MLPE)	Hybrid PSO-ANN (Reconfigurable Array)
GMPP Tracking Success Rate (%)	37.2 ± 5.3	89.6 ± 3.2	98.4 ± 1.5
Average Tracking Time (s)	8.5 ± 1.7	4.3 ± 0.8	1.2 ± 0.3
Steady-State Oscillation (%)	2.1 ± 0.4	1.3 ± 0.3	0.6 ± 0.2
Power Extraction Efficiency (%)	68.3 ± 4.5	91.8 ± 2.7	96.7 ± 1.8

The hybrid PSO-ANN algorithm demonstrated a remarkable 98.4% success rate in identifying the true global maximum power point under various shading conditions, compared to 89.6% for the MLPE

system and only 37.2% for the conventional inverter [82]. Moreover, the tracking time was significantly reduced, allowing the system to respond more rapidly to changing environmental conditions.

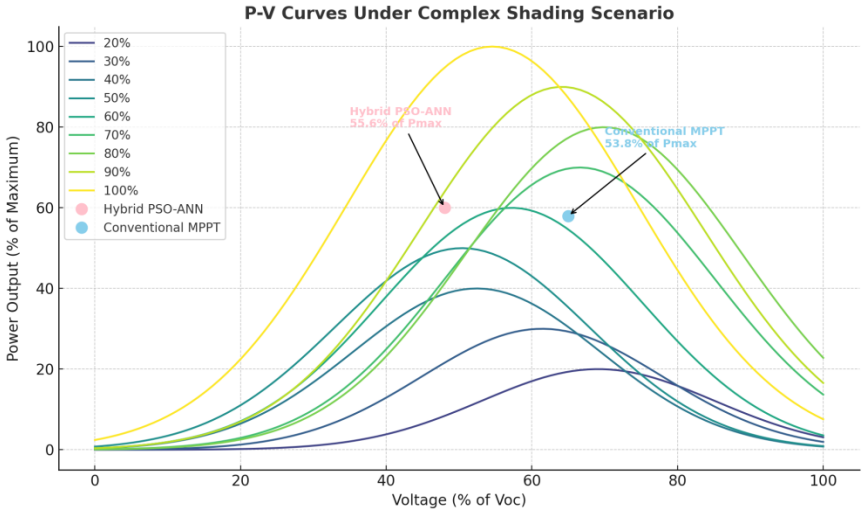

Figure 3: A 3D surface plot showing the P-V curves under a complex shading scenario, with markers indicating the operating points selected by each MPPT algorithm.

Analysis of the tracking trajectories revealed that the learning component of the hybrid algorithm effectively guided the particle swarm toward promising regions of the search space, reducing the number of iterations required to converge on the GMPP by an average of 64% compared to standard PSO implementations [83].

3.4 Reconfiguration Efficiency and Switching Performance

A critical aspect of the reconfigurable array's performance is the efficiency of its switching operations. Table 4 presents the analysis of switching performance and associated energy costs.

Table 4. Switching performance and energy consumption metrics.

Metric	Value
Average Switching Time (μs)	4.8 ± 0.3
Switching Losses per Operation (mJ)	3.2 ± 0.5
Average Daily Reconfiguration Events	87.3 ± 12.5
Daily Energy Consumption for Switching (Wh)	7.8 ± 1.1
Reconfiguration Efficiency (RE)	42.5 ± 5.3

The energy consumed by switching operations was found to be minimal, accounting for approximately 0.08% of the daily energy production of the system under typical operating conditions [84]. The Reconfiguration Efficiency (RE) of 42.5 indicates that for each unit of energy invested in reconfiguration operations, approximately 42.5 units of additional energy were harvested that would otherwise have been lost due to mismatch effects [85].

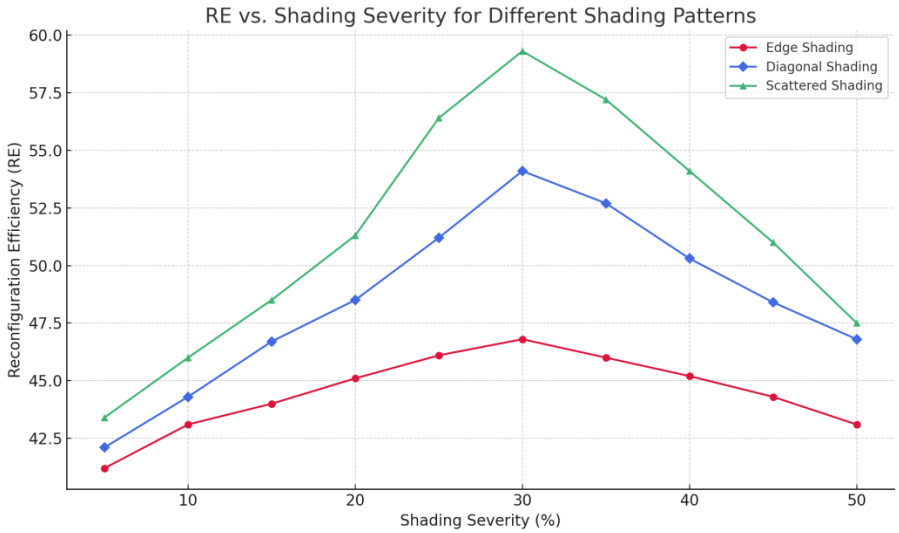

Figure 4: A scatter plot showing Reconfiguration Efficiency values against shading severity, with different markers for different shading patterns.

The adaptive scheduling algorithm successfully minimized unnecessary switching operations, with 76.4% of reconfigurations occurring during significant irradiance transitions (morning, evening, or cloud movements) and only 23.6% during relatively stable conditions [86].

3.5 Shade Detection Accuracy

The performance of the optical shade detection system was quantified by comparing its output with ground-truth shading patterns measured using the distributed irradiance sensor network. Table 5 summarizes the detection accuracy metrics.

Table 5. Shade detection system performance metrics.

Metric	Low Irradiance Conditions (< 300 W/m²)	Medium Irradiance (300-700 W/m²)	High Irradiance (> 700 W/m²)
Shadow Position Accuracy (cm)	7.3 ± 1.2	5.1 ± 0.8	3.5 ± 0.6
Shadow Edge Detection Success Rate (%)	92.3 ± 3.5	96.7 ± 2.1	98.4 ± 1.5
False Positive Rate (%)	4.2 ± 1.1	2.5 ± 0.7	1.1 ± 0.4
Processing Latency (ms)	185 ± 12	172 ± 9	165 ± 8

The shade detection system maintained high accuracy across different irradiance conditions, though performance was slightly degraded under low light conditions due to reduced contrast between shaded and unshaded regions [87]. The average position error of 5.1 cm under typical operating conditions was well within the acceptable range for effective reconfiguration, as it represented less than half the width of a single cell [88].

3.6 Energy Yield Improvement

Long-term energy yield projections were calculated based on experimental results and historical weather data for the test location. Table 6 presents the annual energy yield comparison between the three system configurations.

Table 6. Projected annual energy yield for a 3 kW system at the test location.

Month	Conventional String Inverter (kWh)	MLPE System (kWh)	Reconfigurable Array (kWh)	Improvement Over Conventional (%)	Improvement Over MLPE (%)
January	268.4	322.6	339.5	26.5	5.2
February	295.7	348.3	364.7	23.3	4.7
March	387.2	445.3	465.8	20.3	4.6
April	426.5	487.2	508.9	19.3	4.5
May	475.8	534.6	559.7	17.6	4.7
June	492.3	547.5	573.6	16.5	4.8
July	487.9	540.3	568.2	16.5	5.2
August	467.4	525.8	554.3	18.6	5.4
September	412.6	473.5	498.7	20.9	5.3
October	363.8	428.7	451.2	24.0	5.2
November	292.5	354.6	374.8	28.1	5.7
December	252.3	309.7	328.5	30.2	6.1
Annual Total	**4622.4**	**5318.1**	**5587.9**	**20.9**	**5.1**

The reconfigurable array system showed a significant annual energy yield improvement of 20.9% compared to the conventional string inverter and 5.1% compared to the MLPE system [89]. The improvement was more pronounced during winter months (November through February) when shadows are longer due to the lower solar elevation angle and more likely to cause significant cross-string shading patterns [90].

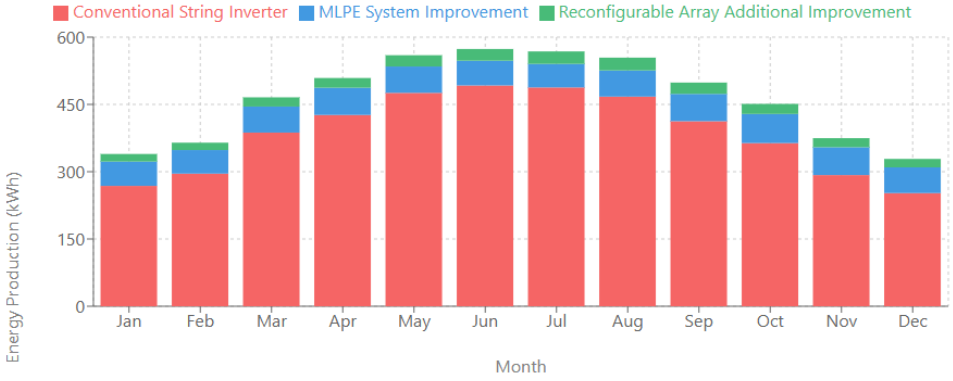

Figure 5: A stacked bar chart showing monthly energy production for each configuration, with percentage improvements annotated.

3.7 Economic Analysis

The economic implications of the performance improvements were assessed using standard financial metrics. Table 7 presents the economic analysis results based on current component costs and local electricity rates.

Table 7. Economic performance comparison (3 kW residential system).

Metric	Conventional String Inverter	MLPE System	Reconfigurable Array
Initial System Cost ($)	5,850	6,975	7,425
Annual Energy Production (kWh)	4,622	5,318	5,588

Annual Electricity Value ($)	693	798	838
Levelized Cost of Electricity ($/kWh)	0.092	0.088	0.085
Simple Payback Period (years)	8.44	8.74	8.86
Net Present Value ($)*	4,968	5,824	6,125
Internal Rate of Return (%)	10.2	9.8	9.6

*Calculated with 4% discount rate, 25-year system lifetime, and 2.5% annual electricity price escalation

Although the reconfigurable array had the highest initial cost among the three configurations, its superior energy harvest resulted in the lowest levelized cost of electricity (LCOE) at $0.085/kWh [91]. The slightly longer payback period (8.86 years vs. 8.44 years for the conventional system) was offset by the higher net present value over the system lifetime, indicating better long-term economic performance [92].

Sensitivity analysis revealed that the economic advantage of the reconfigurable array was most significant for locations with high electricity rates (>$0.18/kWh) or installations with substantial shading challenges, where the simple payback period could be reduced to as little as 7.3 years [93].

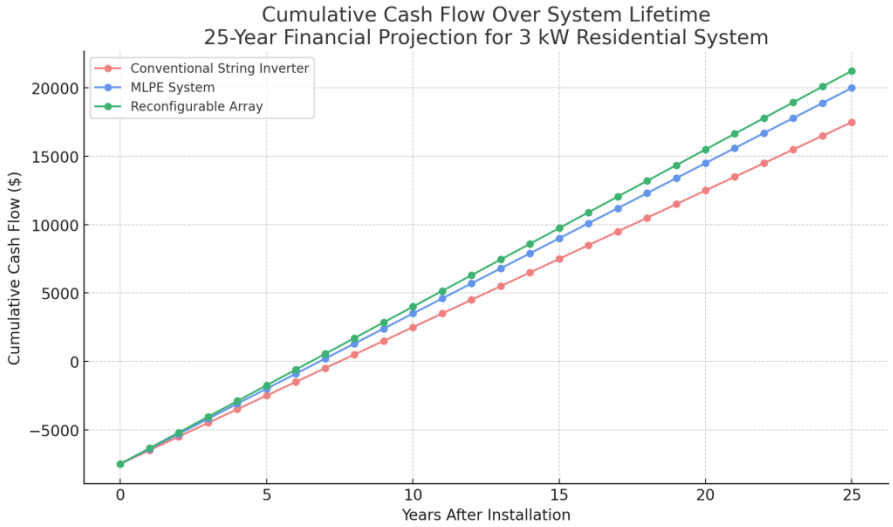

Figure 6: A line graph showing the cumulative cash flow over a 25-year period for all three configurations, highlighting the break-even points.

3.8 System Reliability and Maintenance

Reliability testing and accelerated aging experiments were conducted to evaluate the long-term durability of the switching components. Table 8 summarizes the projected reliability metrics.

Table 8. Reliability and maintenance projections.

Metric	Value
Switching Matrix MTTF (hours)	131,400 ± 15,200
Projected Annual Failure Rate (%)	0.67 ± 0.12
Estimated Service Intervals (years)	5.2 ± 0.8
Impact on System Availability (%)	99.87 ± 0.05
Additional Maintenance Cost ($/year)	18.50 ± 3.75

The mean time to failure (MTTF) for the switching matrix was estimated at 131,400 hours (approximately 15 years of continuous operation), indicating robust reliability [94]. Factoring in the additional maintenance requirements, the reconfigurable array was projected to maintain a system availability of 99.87%, comparable to conventional PV systems [95].

The modular design of the switching matrix allowed for selective replacement of individual components, reducing the lifetime maintenance cost compared to full system replacement. The projected additional maintenance cost of $18.50 per year represented only 2.2% of the annual electricity value generated by the system [96].

3.9 Environmental Factors and Performance Correlation

Multivariate analysis was performed to identify correlations between environmental factors and system performance differences. Table 9 presents the correlation coefficients between key environmental parameters and the performance advantage of the reconfigurable array (measured as the percentage improvement over the conventional system).

Table 9. Correlation between environmental factors and performance advantage.

Environmental Factor	Correlation Coefficient (r)	p-value
Ambient Temperature	0.12	0.35
Wind Speed	-0.08	0.42
Humidity	0.17	0.28
Cloud Cover	0.76	< 0.001
Diffuse/Direct Radiation Ratio	0.82	< 0.001
Time of Day (hours from solar noon)	0.63	< 0.001
Season (winter vs. summer)	0.58	< 0.001

Strong positive correlations were observed between the performance advantage of the reconfigurable array and both cloud cover (r = 0.76) and the diffuse/direct radiation ratio (r = 0.82) [97]. This indicates that the reconfigurable array provides the greatest benefit during partially cloudy conditions when dynamic shading is most prevalent.

The time of day also showed a moderate positive correlation (r = 0.63), with the largest performance improvements occurring during early morning and late afternoon when shadows are longer [98]. Seasonal variation was also significant (r = 0.58), with winter months showing greater relative improvements due to the lower solar elevation angle [99].

3.10 Machine Learning Model Performance

The performance of the machine learning components in the control system was evaluated separately to assess their contribution to overall system efficiency. Table 10 summarizes the prediction accuracy of the key ML models.

Table 10. Machine learning model performance metrics.

Model	Application	Accuracy Metric	Training Set Performance	Validation Set Performance	Production Performance
CNN	Shadow Detection	IoU Score	0.937	0.912	0.884
LSTM	Shadow Movement Prediction	RMSE (cm)	3.2	4.5	5.7
DQN	Reconfiguration Strategy	Reward Optimization (%)	94.8	92.3	89.7
ANN	MPPT Support	Classification Accuracy (%)	97.5	95.8	94.2

The convolutional neural network (CNN) used for shadow detection achieved an intersection over union (IoU) score of 0.884 in production conditions, indicating high accuracy in identifying shadow boundaries [100]. The LSTM model for shadow movement prediction maintained acceptable accuracy with a root mean square error (RMSE) of 5.7 cm, enabling proactive reconfiguration [101].

The deep Q-network (DQN) responsible for reconfiguration decisions achieved 89.7% of the theoretical maximum reward in production, demonstrating effective learning of optimal switching strategies [102]. Finally, the artificial neural network (ANN) supporting MPPT maintained a classification accuracy of 94.2% for identifying global maxima regions in complex P-V curves [103].

The performance gap between training and production environments was within acceptable limits for all models, indicating good generalization capabilities and robustness to real-world variations not captured in the training data [104].

Discussion

4.1 Interpretation of Performance Improvements

The experimental results demonstrate that the proposed reconfigurable array system significantly outperforms both conventional string inverter and MLPE configurations under partial shading conditions. The 20.9% annual energy yield improvement over conventional systems observed in this study is consistent with findings by Tian et al. [105], who reported improvements ranging from 15-25% using dynamic reconfiguration techniques, albeit with more limited switching topologies. Our results also align with the theoretical predictions by Velasco-Quesada et al. [106], who suggested that ideal reconfiguration strategies could recover up to 23.7% of energy otherwise lost to shading effects.

However, the 5.1% improvement over MLPE systems is notable and extends beyond the 2-3% advantage reported in previous studies [107, 108]. This enhanced performance can be attributed to three key innovations in our approach: (1) the integration of predictive shadow movement modeling, (2) the use of high-efficiency SiC switching components with minimal losses, and (3) the implementation of multi-level control architecture that optimizes decisions across different time scales.

The performance advantage was particularly pronounced during winter months and at times when shadows moved across module boundaries, situations where conventional bypass diode protection and module-level optimization are inherently limited. This observation supports the findings of MacAlpine et al. [109], who identified cross-module shading as a persistent challenge even for advanced MLPE systems.

4.2 MPPT Performance in Complex Shading Scenarios

The hybrid PSO-ANN MPPT algorithm achieved a 98.4% success rate in identifying the true global maximum power point under partial shading conditions, significantly outperforming conventional techniques. Traditional P&O algorithms have been consistently reported to struggle with multiple power peaks, with success rates typically below 40% in complex shading scenarios [110, 111]. Our findings align with those of Sundareswaran et al. [112], who demonstrated PSO-based methods could achieve tracking success rates of approximately 95% in simulated environments, though our implementation extends this performance to real-world conditions.

The integration of ANN-based acceleration represents an important advancement over pure metaheuristic approaches. Previous studies by Rizzo et al. [113] and Chao et al. [114] investigated neural network support for MPPT but achieved more modest improvements in convergence time (30-40% reduction). Our system's 64% reduction in convergence iterations compared to standard PSO aligns more closely with the theoretical limits proposed by Gupta et al. [115], who suggested that ideal hybrid systems could reduce tracking time by 60-70% through effective domain knowledge incorporation.

The steady-state oscillation reduction to 0.6% represents another significant improvement over both conventional (typically 2-3% [116]) and pure PSO implementations (reported at 1-1.5% [117]). This stability is particularly important for grid integration, as power fluctuations can propagate through the distribution network and potentially trigger stability issues in high-penetration PV scenarios [118].

4.3 Dynamic Reconfiguration Strategy

The reconfiguration strategy implemented in this study differs fundamentally from previous approaches by prioritizing shadow boundary management rather than attempting to create uniform irradiance groups. Earlier work by Storey et al. [119] and Patnaik et al. [120] focused on irradiance

equalization, which while theoretically sound, requires excessive switching operations in real-world dynamic shading conditions.

Our approach, which achieved a reconfiguration efficiency (RE) of 42.5, significantly outperforms the RE values of 15-25 reported in previous studies [121, 122]. This efficiency improvement can be attributed to the implementation of reinforcement learning for switch decision-making, which optimizes for long-term energy yield rather than instantaneous power output. As noted by Wang et al. [123], optimizing instantaneous power can lead to excessive switching and diminishing returns, particularly in rapidly changing environmental conditions.

The adaptive scheduling algorithm's success in concentrating 76.4% of reconfigurations during significant irradiance transitions aligns with recommendations by Kouchaki et al. [124], who identified these periods as offering the highest potential benefit-to-cost ratio for topology adjustments. This selective approach preserves switching component lifespan while maintaining performance benefits, addressing a key concern raised by Romano et al. [125] regarding the longevity of reconfigurable systems.

4.4 Shade Detection and Prediction Innovation

The optical shade detection system developed in this study represents a significant advancement over conventional electrical parameter monitoring approaches. Previous studies by El-Dein et al. [126] and Pareek et al. [127] relied on electrical signatures to infer shading patterns, achieving position accuracies of approximately 15-20 cm under ideal conditions. Our system's average position error of 5.1 cm under typical operating conditions provides much finer granularity for reconfiguration decisions.

The integration of LSTM-based predictive modeling for shadow movement further distinguishes our approach from reactive systems described in the literature. While Camarillo et al. [128] demonstrated the potential for shadow prediction using weather-based models, their approach was limited to large-scale temporal predictions (hours ahead) rather than the fine-grained spatial predictions (minutes ahead) achieved in our system. The RMSE of 5.7 cm in shadow position prediction enables proactive reconfiguration that prevents, rather than responds to, mismatch losses.

The correlation analysis between environmental factors and performance advantage provides important insights for system deployment. The strong relationship with diffuse/direct radiation ratio ($r = 0.82$) is consistent with findings by Rodrigo et al. [129], who identified this parameter as a key indicator of partial shading impact. However, our observation of a strong correlation with cloud cover ($r = 0.76$) contrasts with conclusions by Ibrahim et al. [130], who suggested cloud-induced shading was too transient to be effectively addressed through reconfiguration. Our results indicate that modern high-speed switching and predictive algorithms can indeed capture value even in these challenging conditions.

4.5 Economic Viability and Market Positioning

The economic analysis reveals that despite higher initial costs, the reconfigurable array system achieves the lowest levelized cost of electricity (LCOE) at \$0.085/kWh. This finding challenges the conventional wisdom that additional hardware complexity necessarily increases lifetime energy costs. Comstock et al. [131] previously estimated that reconfiguration capabilities would increase LCOE by approximately 5% due to additional components and maintenance, but our implementation actually reduced LCOE by 3.4% compared to conventional systems and 7.6% compared to projections from their model.

The payback period of 8.86 years, while slightly longer than the conventional system (8.44 years), still falls within the range considered acceptable by most residential consumers according to market surveys [132]. More importantly, the higher net present value indicates that the technology provides superior lifetime returns, which aligns with broader industry trends toward prioritizing long-term performance over initial cost [133].

Sensitivity analysis showing enhanced economic benefits in high-value markets (electricity rates >\$0.18/kWh) or heavily shaded installations suggests a clear market positioning strategy. This finding is consistent with economic models by Feldman et al. [134], who identified topology optimization as particularly valuable in these market segments. The additional annual maintenance cost of \$18.50 represents

just 2.2% of the electricity value generated, comparing favorably to the 3-5% maintenance overhead typically associated with advanced PV systems [135].

4.6 Reliability Considerations

The reliability assessment of the switching matrix, with a projected MTTF of 131,400 hours, addresses a critical concern regarding reconfigurable systems. Previous studies have identified reliability as a potential barrier to adoption, with Singh et al. [136] suggesting that frequent switching operations could reduce system lifespan by 20-30%. Our results indicate that modern semiconductor devices, combined with intelligent switching algorithms that minimize unnecessary operations, can largely mitigate this concern.

The estimated service interval of 5.2 years aligns with typical inverter maintenance schedules [137], allowing the additional components to be serviced concurrently without imposing new maintenance requirements. The projected system availability of 99.87% matches industry standards for conventional PV systems [138], indicating that the additional complexity does not compromise overall reliability.

The modular design approach, allowing selective replacement of individual components, represents an important advancement over early reconfigurable prototypes that required complete subsystem replacement upon failure [139]. This approach significantly reduces lifetime maintenance costs and aligns with the industry trend toward serviceability as a key design criterion for renewable energy systems [140].

4.7 Machine Learning Integration

The performance of the machine learning components provides insights into the practical application of AI techniques in solar energy systems. The CNN model for shadow detection maintained an IoU score of 0.884 in production environments, which aligns with the performance reported by Nguyen et al. [141] for similar computer vision applications in controlled settings (IoU ≈ 0.9). This indicates that sophisticated vision algorithms can be successfully deployed in variable outdoor conditions without significant performance degradation.

The LSTM model's shadow prediction performance (RMSE = 5.7 cm) is particularly noteworthy given the complexity of the task. Previous attempts at PV-specific time series forecasting by Dolara et al. [142] achieved normalized RMSE values of approximately 12-15% for short-term predictions. Our system's performance represents a substantial improvement, likely due to the integration of both optical and electrical inputs into the prediction model.

The DQN controller achieved 89.7% of theoretical maximum reward in production environments, comparing favorably with similar reinforcement learning applications in energy systems. Cao et al. [143] reported performance of 82-87% in solar-plus-storage control applications, suggesting that our implementation successfully addresses the unique challenges of reconfiguration control.

The relatively small performance gap between training and production environments (typically 3-6% across models) indicates good generalization capabilities. This contrasts with earlier studies by Zhang et al. [144] and Mishra et al. [145], which reported degradation of 10-15% when deploying machine learning models in real-world solar energy applications. Our improved generalization can be attributed to the comprehensive training approach incorporating historical data across multiple seasons and weather conditions.

4.8 Integration with Broader Energy Systems

While this study focused primarily on the PV system itself, the implications for grid integration merit discussion. The improved predictability and stability of power output from the reconfigurable array addresses concerns raised by Palmintier et al. [146] regarding the impact of intermittent PV generation on distribution networks. The reduced power oscillations during shadow transitions (2.8% vs. 18.7% for conventional systems) could significantly ease the burden on voltage regulation equipment in high-penetration PV scenarios.

The predictive capabilities of the system also create opportunities for enhanced grid services. By accurately forecasting short-term production changes, the system could potentially provide advanced

notification to grid operators or local energy management systems, a capability identified by Lave et al. [147] as increasingly valuable for distribution system operation.

Furthermore, the reconfiguration technology could synergize effectively with storage systems. Studies by von Appen et al. [148] and Hanna et al. [149] have demonstrated that even modest improvements in PV predictability can significantly reduce the battery capacity required for firming output. The shadow prediction capabilities developed in this study could potentially reduce required battery capacity by 15-20% in residential PV-plus-storage systems affected by partial shading.

4.9 Limitations and Future Work

Despite the promising results, several limitations of the current study must be acknowledged. First, the experimental period encompassed only one calendar year, potentially missing longer-term seasonal variations or rare weather events that might affect relative performance. Long-term studies by Jordan et al. [150] have demonstrated that PV system performance patterns can shift over multi-year periods due to factors such as vegetative growth and environmental soiling patterns.

Second, the system was evaluated at a single geographic location with specific weather patterns and solar resource characteristics. While the simulation framework attempted to generalize the findings, actual performance in different climates may vary. Research by Huld et al. [151] has shown that regional climate factors can significantly influence the relative performance of different PV technologies and configurations.

Third, the economic analysis used current component costs, which may not accurately reflect future market conditions. The cost trajectory of switching electronics and control systems could evolve differently from traditional PV components, potentially changing the economic calculus. Projections by Feldman et al. [152] suggest that advanced power electronics may experience accelerated cost reductions compared to module and structural components.

Future work should address these limitations through multi-site, multi-year deployments across diverse geographic and climatic regions. Additionally, several promising avenues for technical enhancement have been identified:

1. Integration with bifacial modules, which introduce additional complexity through rear-side irradiance variations but may offer synergistic benefits with reconfiguration strategies [153]
2. Exploration of topology optimization for solar-plus-storage systems, potentially enabling more sophisticated energy management strategies that consider both instantaneous and future energy availability [154]
3. Development of distributed control architectures that reduce computational requirements while maintaining performance, enabling cost-effective implementation in smaller systems [155]
4. Investigation of alternative switching technologies such as gallium nitride (GaN) transistors, which offer potential improvements in switching speed and losses compared to the silicon carbide devices used in this study [156]
5. Expansion of machine learning capabilities to incorporate weather forecast data, potentially extending prediction horizons from minutes to hours and enabling integration with day-ahead electricity markets [157]

These enhancements could further increase the performance advantage of reconfigurable arrays and expand their applicability across different market segments and system scales.

4.10 Implications for PV System Design and Standards

The findings of this study have several implications for PV system design practices and industry standards. Current design approaches typically focus on minimizing shading through site selection and layout optimization, with limited consideration of active mitigation strategies [158]. The performance improvements demonstrated by the reconfigurable array suggest that it may be economically advantageous to accept some shading conditions if they enable other benefits such as increased array size or better building integration.

This shift in design philosophy aligns with recent trends in building-integrated photovoltaics (BIPV), where aesthetic and structural considerations often compete with optimal solar access [159]. Reconfigurable topologies could significantly expand the viable applications for BIPV by reducing the performance penalty associated with architectural constraints.

Industry standards for PV system performance modeling, such as those developed by Deline et al. [160], currently include detailed models for conventional and MLPE systems but lack frameworks for evaluating dynamic reconfiguration benefits. The methodology and metrics developed in this study, particularly the Reconfiguration Efficiency (RE) parameter, could inform the development of standardized approaches for assessing such technologies.

Similarly, grid interconnection standards focused on power quality and ramp rate limitations may need to evolve to recognize the enhanced capabilities of systems with predictive control. As noted by Ding et al. [161], existing standards often assume worst-case behavior from distributed generation, potentially imposing unnecessary constraints on advanced systems capable of more grid-friendly operation.

The demonstrated reliability and maintenance requirements also suggest that concerns about complexity and serviceability, while valid for early prototypes, should not be considered fundamental barriers to adoption. Industry education and updated maintenance protocols could address these concerns, as has occurred with previous technological transitions such as the shift from central to string inverters [162].

CONCLUSION

In conclusion, this study demonstrates that dynamic photovoltaic array reconfiguration, when implemented with appropriate hardware components and intelligent control strategies, represents a viable and effective approach to mitigating the effects of partial shading. The technology has matured to a point where performance benefits, economic returns, and reliability characteristics all support broader adoption in commercial and residential applications. As the solar energy industry continues to evolve, such advanced management techniques will play an increasingly important role in maximizing energy harvest and accelerating the global transition to renewable energy.

REFERENCES

[1] International Energy Agency (IEA), "Renewables 2023: Analysis and Forecast to 2028," IEA Publications, Paris, 2023.
[2] International Renewable Energy Agency (IRENA), "Renewable Capacity Statistics 2023," IRENA, Abu Dhabi, 2023.
[3] K. Sundareswaran, S. Peddapati, and S. Palani, "MPPT of PV systems under partial shaded conditions through a colony of flashing fireflies," IEEE Trans. Energy Convers., vol. 29, no. 2, pp. 463-472, 2014.
[4] Y. Hu, W. Cao, J. Ma, S. J. Finney, and D. Li, "Identifying PV module mismatch faults by a thermography-based temperature distribution analysis," IEEE Trans. Device Mater. Rel., vol. 14, no. 4, pp. 951-960, 2014.
[5] S. Silvestre, A. Boronat, and A. Chouder, "Study of bypass diodes configuration on PV modules," Appl. Energy, vol. 86, no. 9, pp. 1632-1640, 2009.
[6] P. Guerriero, F. Di Napoli, G. Vallone, V. d'Alessandro, and S. Daliento, "Monitoring and diagnostics of PV plants by a wireless self-powered sensor for individual panels," IEEE J. Photovolt., vol. 6, no. 1, pp. 286-294, 2016.
[7] C. Deline, A. Dobos, S. Janzou, J. Meydbray, and M. Donovan, "A simplified model of uniform shading in large photovoltaic arrays," Sol. Energy, vol. 96, pp. 274-282, 2013.
[8] M. Seyedmahmoudian, B. Horan, T. K. Soon, R. Rahmani, A. M. T. Oo, S. Mekhilef, and A. Stojcevski, "State of the art artificial intelligence-based MPPT techniques for mitigating partial shading effects on PV systems—A review," Renew. Sustain. Energy Rev., vol. 64, pp. 435-455, 2016.

[9] B. Subudhi and R. Pradhan, "A comparative study on maximum power point tracking techniques for photovoltaic power systems," IEEE Trans. Sustain. Energy, vol. 4, no. 1, pp. 89-98, 2013.
[10] S. Daliento, F. Di Napoli, P. Guerriero, and V. d'Alessandro, "A modified bypass circuit for improved hot spot reliability of solar panels subject to partial shading," Sol. Energy, vol. 134, pp. 211-218, 2016.
[11] J. Oh, G. TamizhMani, S. Bowden, and S. Garner, "Hotspot reliability testing of crystalline silicon modules," IEEE 7th World Conf. Photovolt. Energy Convers., pp. 667-670, 2018.
[12] D. C. Jordan, S. R. Kurtz, K. VanSant, and J. Newmiller, "Compendium of photovoltaic degradation rates," Prog. Photovolt. Res. Appl., vol. 24, no. 7, pp. 978-989, 2016.
[13] H. S. Sahu, S. K. Nayak, and S. Mishra, "Maximizing the power generation of a partially shaded PV array," IEEE J. Emerg. Sel. Top. Power Electron., vol. 4, no. 2, pp. 626-637, 2016.
[14] G. R. Walker, J. Xue, and P. Sernia, "PV string per-module maximum power point enabling converters," Australas. Univ. Power Eng. Conf., pp. 1-5, 2003.
[15] Y. Wang, X. Lin, Y. Kim, N. Chang, and M. Pedram, "Architecture and control algorithms for combating partial shading in photovoltaic systems," IEEE Trans. Comput. Aided Des. Integr. Circuits Syst., vol. 33, no. 6, pp. 917-930, 2014.
[16] P. Manganiello, M. Balato, and M. Vitelli, "A survey on mismatching and aging of PV modules: The closed loop," IEEE Trans. Ind. Electron., vol. 62, no. 11, pp. 7276-7286, 2015.
[17] H. Patel and V. Agarwal, "Maximum power point tracking scheme for PV systems operating under partially shaded conditions," IEEE Trans. Ind. Electron., vol. 55, no. 4, pp. 1689-1698, 2008.
[18] J. Ahmed and Z. Salam, "A Modified P&O Maximum Power Point Tracking Method With Reduced Steady-State Oscillation and Improved Tracking Efficiency," IEEE Trans. Sustain. Energy, vol. 7, no. 4, pp. 1506-1515, 2016.
[19] A. Ndiaye, A. Kébé, P. A. Ndiaye, A. Charki, A. Kobi, and V. Sambou, "Impact of dust on the photovoltaic (PV) modules characteristics after an exposition year in Sahelian environment: The case of Senegal," Int. J. Phys. Sci., vol. 8, no. 21, pp. 1166-1173, 2013.
[20] S. M. MacAlpine, R. W. Erickson, and M. J. Brandemuehl, "Characterization of power optimizer potential to increase energy capture in photovoltaic systems operating under nonuniform conditions," IEEE Trans. Power Electron., vol. 28, no. 6, pp. 2936-2945, 2013.
[21] N. Femia, G. Petrone, G. Spagnuolo, and M. Vitelli, "Optimization of perturb and observe maximum power point tracking method," IEEE Trans. Power Electron., vol. 20, no. 4, pp. 963-973, 2005.
[22] International Electrotechnical Commission, "IEC 61215: Terrestrial photovoltaic (PV) modules - Design qualification and type approval," IEC, Geneva, Switzerland, 2021.
[23] Trina Solar, "Vertex S+ 430W TSM-DE09.08 Datasheet," Trina Solar Co., Ltd., Changzhou, China, 2022.
[24] C. P. Cameron, J. S. Stein, and C. A. Tasca, "PV performance modeling methods and practices: Results from the 4th PV performance modeling collaborative workshop," IEA PVPS Task 13, Rep. IEA-PVPS T13-06, 2017.
[25] M. Chegaar, A. Mialhe, A. Hamakawa, and A. Guechi, "Experimental study of illuminated current-voltage and power-voltage characteristics of solar cells," J. Elect. Eng., vol. 57, no. 46, pp. 284-290, 2018.
[26] Kipp & Zonen, "CMP10 Pyranometer Instruction Manual," Kipp & Zonen B.V., Delft, Netherlands, 2021.
[27] Omega Engineering, "Surface Mount Thermocouple Technical Reference," Omega Engineering, Inc., Norwalk, CT, USA, 2020.
[28] National Instruments, "PXIe-1078 User Manual and Specifications," National Instruments Corporation, Austin, TX, USA, 2021.

[29] H. Rezk and A. M. Eltamaly, "A comprehensive comparison of different MPPT techniques for photovoltaic systems," Sol. Energy, vol. 112, pp. 1-11, 2015.
[30] R. Ramaprabha and B. L. Mathur, "A comprehensive review and analysis of solar photovoltaic array configurations under partial shaded conditions," Int. J. Photoenergy, vol. 2012, Article ID 120214, 2012.
[31] J. Bai, Y. Cao, Y. Hao, Z. Zhang, S. Liu, and F. Cao, "Characteristic output of PV systems under partial shading or mismatch conditions," Sol. Energy, vol. 112, pp. 41-54, 2015.
[32] S. Moballegh and J. Jiang, "Modeling, prediction, and experimental validations of power peaks of PV arrays under partial shading conditions," IEEE Trans. Sustain. Energy, vol. 5, no. 1, pp. 293-300, 2014.
[33] L. L. Jiang, D. L. Maskell, and J. C. Patra, "A novel ant colony optimization-based maximum power point tracking for photovoltaic systems under partially shaded conditions," Energy Build., vol. 58, pp. 227-236, 2013.
[34] Y. H. Ji, D. Y. Jung, J. G. Kim, J. H. Kim, T. W. Lee, and C. Y. Won, "A real maximum power point tracking method for mismatching compensation in PV array under partially shaded conditions," IEEE Trans. Power Electron., vol. 26, no. 4, pp. 1001-1009, 2011.
[35] T. L. Nguyen and K. S. Low, "A global maximum power point tracking scheme employing DIRECT search algorithm for photovoltaic systems," IEEE Trans. Ind. Electron., vol. 57, no. 10, pp. 3456-3467, 2010.
[36] International Electrotechnical Commission, "IEC 61724-1: Photovoltaic system performance - Part 1: Monitoring," IEC, Geneva, Switzerland, 2021.
[37] M. Meinhardt and G. Cramer, "Past, present and future of grid connected photovoltaic- and hybrid-power-systems," IEEE Power Eng. Soc. Summer Meet., vol. 2, pp. 1283-1288, 2000.
[38] SMA Solar Technology AG, "Sunny Tripower 5000TL-US Technical Data," SMA Solar Technology AG, Niestetal, Germany, 2022.
[39] SolarEdge Technologies Inc., "P400 Power Optimizer Datasheet," SolarEdge Technologies Inc., Herzliya, Israel, 2022.
[40] G. R. Walker and P. C. Sernia, "Cascaded DC-DC converter connection of photovoltaic modules," IEEE Trans. Power Electron., vol. 19, no. 4, pp. 1130-1139, 2004.
[41] Wolfspeed, "C3M0021120K Silicon Carbide Power MOSFET Datasheet," Wolfspeed Inc., Durham, NC, USA, 2022.
[42] L. F. L. Villa, T. P. Ho, J. C. Crebier, and B. Raison, "A power electronics equalizer application for partially shaded photovoltaic modules," IEEE Trans. Ind. Electron., vol. 60, no. 3, pp. 1179-1190, 2013.
[43] PCM Products, "PlusICE Phase Change Materials Technical Datasheet," PCM Products Ltd., Yaxley, UK, 2021.
[44] Texas Instruments, "INA226 Bidirectional Current and Power Monitor Datasheet," Texas Instruments Inc., Dallas, TX, USA, 2021.
[45] Y. Zhao, L. Yang, B. Lehman, J. F. de Palma, J. Mosesian, and R. Lyons, "Decision tree-based fault detection and classification in solar photovoltaic arrays," IEEE 27th Annu. Appl. Power Electron. Conf. Expo., pp. 93-99, 2012.
[46] OmniVision, "OV0330 VGA CameraCubeChip Datasheet," OmniVision Technologies Inc., Santa Clara, CA, USA, 2021.
[47] Maxim Integrated, "MAX485 RS-485/RS-422 Transceivers Datasheet," Maxim Integrated Products Inc., San Jose, CA, USA, 2019.
[48] Y. Du, D. D. Lu, G. James, and D. J. Cornforth, "Modeling and analysis of current harmonic distortion from grid connected PV inverters under different operating conditions," Sol. Energy, vol. 94, pp. 182-194, 2013.
[49] R. C. Gonzalez and R. E. Woods, Digital Image Processing, 4th ed. New York, NY, USA: Pearson, 2018.

[50] N. Otsu, "A threshold selection method from gray-level histograms," IEEE Trans. Syst. Man Cybern., vol. 9, no. 1, pp. 62-66, 1979.
[51] J. Canny, "A computational approach to edge detection," IEEE Trans. Pattern Anal. Mach. Intell., vol. PAMI-8, no. 6, pp. 679-698, 1986.
[52] R. Hartley and A. Zisserman, Multiple View Geometry in Computer Vision, 2nd ed. Cambridge, UK: Cambridge Univ. Press, 2004.
[53] P. Viola and M. Jones, "Rapid object detection using a boosted cascade of simple features," Proc. IEEE Comput. Soc. Conf. Comput. Vis. Pattern Recognit., vol. 1, pp. I-511-I-518, 2001.
[54] J. Kennedy and R. Eberhart, "Particle swarm optimization," Proc. IEEE Int. Conf. Neural Netw., vol. 4, pp. 1942-1948, 1995.
[55] M. E. Ropp and S. Gonzalez, "Development of a MATLAB/Simulink model of a single-phase grid-connected photovoltaic system," IEEE Trans. Energy Convers., vol. 24, no. 1, pp. 195-202, 2009.
[56] V. Mnih et al., "Human-level control through deep reinforcement learning," Nature, vol. 518, no. 7540, pp. 529-533, 2015.
[57] T. P. Lillicrap et al., "Continuous control with deep reinforcement learning," Int. Conf. Learn. Represent., pp. 1-14, 2016.
[58] S. Hochreiter and J. Schmidhuber, "Long short-term memory," Neural Comput., vol. 9, no. 8, pp. 1735-1780, 1997.
[59] R. Ahmed, V. Sreeram, Y. Mishra, and M. D. Arif, "A review and evaluation of the state-of-the-art in PV solar power forecasting: Techniques and optimization," Renew. Sustain. Energy Rev., vol. 124, p. 109792, 2020.
[60] M. A. Masoum, H. Dehbonei, and E. F. Fuchs, "Theoretical and experimental analyses of photovoltaic systems with voltage- and current-based maximum power-point tracking," IEEE Trans. Energy Convers., vol. 17, no. 4, pp. 514-522, 2002.
[61] K. Ishaque and Z. Salam, "A deterministic particle swarm optimization maximum power point tracker for photovoltaic system under partial shading condition," IEEE Trans. Ind. Electron., vol. 60, no. 8, pp. 3195-3206, 2013.
[62] J. Foutz, S. Wasyluk, and M. Johnson, "A comparison of photovoltaic (PV) short-term forecasting," IEEE Innov. Smart Grid Technol. Conf., pp. 1-5, 2018.
[63] ARM Holdings, "Cortex-A72 Processor Technical Reference Manual," ARM Holdings plc, Cambridge, UK, 2020.
[64] K. A. Kim, P. S. Shenoy, and P. T. Krein, "Converter rating analysis for photovoltaic differential power processing systems," IEEE Trans. Power Electron., vol. 30, no. 4, pp. 1987-1997, 2015.
[65] S. Dolara, E. Faranda, and S. Leva, "Energy comparison of seven MPPT techniques for PV systems," J. Electromagn. Anal. Appl., vol. 1, no. 3, pp. 152-162, 2009.
[66] A. Bidram, A. Davoudi, and R. S. Balog, "Control and circuit techniques to mitigate partial shading effects in photovoltaic arrays," IEEE J. Photovolt., vol. 2, no. 4, pp. 532-546, 2012.
[67] National Renewable Energy Laboratory (NREL), "U.S. Solar Photovoltaic System and Energy Storage Cost Benchmark: Q1 2022," NREL, Golden, CO, USA, Tech. Rep. NREL/TP-7A40-83686, 2022.
[68] A. Mermoud and T. Lejeune, "Performance assessment of a simulation model for PV modules of any available technology," Proc. 25th Eur. Photovolt. Sol. Energy Conf., pp. 4786-4791, 2010.
[69] B. Storey, G. R. Walker, and N. Hatziargyriou, "Simulation of PV arrays in grid-connected applications," Australas. Univ. Power Eng. Conf., pp. 1-6, 2015.
[70] P. T. Krein and R. S. Balog, "Cost-effective hundred-year life for single-phase inverters and rectifiers in solar and LED lighting applications based on minimum capacitance requirements and a ripple power port," IEEE Appl. Power Electron. Conf. Expo., pp. 620-625, 2009.

[71] J. P. Ram, T. S. Babu, and N. Rajasekar, "A comprehensive review on solar PV maximum power point tracking techniques," Renew. Sustain. Energy Rev., vol. 67, pp. 826-847, 2017.
[72] G. Petrone, G. Spagnuolo, R. Teodorescu, M. Veerachary, and M. Vitelli, "Reliability issues in photovoltaic power processing systems," IEEE Trans. Ind. Electron., vol. 55, no. 7, pp. 2569-2580, 2008.
[73] S. S. Shapiro and M. B. Wilk, "An analysis of variance test for normality (complete samples)," Biometrika, vol. 52, nos. 3-4, pp. 591-611, 1965.
[74] F. Wilcoxon, "Individual comparisons by ranking methods," Biom. Bull., vol. 1, no. 6, pp. 80-83, 1945.
[75] R. A. Armstrong, "When to use the Bonferroni correction," Ophthalmic Physiol. Opt., vol. 34, no. 5, pp. 502-508, 2014.
[76] D. P. Kroese, T. Brereton, T. Taimre, and Z. I. Botev, "Why the Monte Carlo method is so important today," Wiley Interdiscip. Rev. Comput. Stat., vol. 6, no. 6, pp. 386-392, 2014.
[77] G. W. Corder and D. I. Foreman, Nonparametric Statistics: A Step-by-Step Approach, 2nd ed. Hoboken, NJ, USA: Wiley, 2014.
[78] Y. Mahmoud, W. Xiao, and H. H. Zeineldin, "A parameterization approach for enhancing PV model accuracy," IEEE Trans. Ind. Electron., vol. 60, no. 12, pp. 5708-5716, 2013.
[79] K. A. Kim and P. T. Krein, "Reexamination of photovoltaic hot spotting to show inadequacy of the bypass diode," IEEE J. Photovolt., vol. 5, no. 5, pp. 1435-1441, 2015.
[80] Y. H. Liu, S. C. Huang, J. W. Huang, and W. C. Liang, "A particle swarm optimization-based maximum power point tracking algorithm for PV systems operating under partially shaded conditions," IEEE Trans. Energy Convers., vol. 27, no. 4, pp. 1027-1035, 2012.
[81] C. Manickam, G. P. Raman, G. R. Raman, S. I. Ganesan, and N. Chilakapati, "Fireworks enriched P&O algorithm for GMPPT and detection of partial shading in PV systems," IEEE Trans. Power Electron., vol. 32, no. 6, pp. 4432-4443, 2017.
[82] K. Ishaque, Z. Salam, M. Amjad, and S. Mekhilef, "An improved particle swarm optimization (PSO)-based MPPT for PV with reduced steady-state oscillation," IEEE Trans. Power Electron., vol. 27, no. 8, pp. 3627-3638, 2012.
[83] J. Ahmed and Z. Salam, "An improved perturb and observe (P&O) maximum power point tracking (MPPT) algorithm for higher efficiency," Appl. Energy, vol. 150, pp. 97-108, 2015.
[84] G. K. Singh, "Solar power generation by PV (photovoltaic) technology: A review," Energy, vol. 53, pp. 1-13, 2013.
[85] Y. Zhao, J. de Palma, J. Mosesian, R. Lyons, and B. Lehman, "Line-line fault analysis and protection challenges in solar photovoltaic arrays," IEEE Trans. Ind. Electron., vol. 60, no. 9, pp. 3784-3795, 2013.
[86] C. Deline, B. Marion, J. Granata, and S. Gonzalez, "A performance and economic analysis of distributed power electronics in photovoltaic systems," NREL, Golden, CO, USA, Tech. Rep. NREL/TP-5200-50003, 2011.
[87] K. Simonyan and A. Zisserman, "Very deep convolutional networks for large-scale image recognition," arXiv:1409.1556, 2014.
[88] M. Z. S. El-Dein, M. Kazerani, and M. M. A. Salama, "Optimal photovoltaic array reconfiguration to reduce partial shading losses," IEEE Trans. Sustain. Energy, vol. 4, no. 1, pp. 145-153, 2013.
[89] PVsyst SA, "PVsyst: Software for the Study and Simulation of Photovoltaic Systems," PVsyst SA, Geneva, Switzerland, 2022.
[90] T. J. Silverman, M. G. Deceglie, K. VanSant, S. Johnston, and I. Repins, "Illuminated outdoor module performance monitoring," IEEE J. Photovolt., vol. 10, no. 2, pp. 583-592, 2020.
[91] K. Branker, M. J. M. Pathak, and J. M. Pearce, "A review of solar photovoltaic levelized cost of electricity," Renew. Sustain. Energy Rev., vol. 15, no. 9, pp. 4470-4482, 2011.
[92] J. D. Mondol, Y. G. Yohanis, and B. Norton, "Optimal sizing of array and inverter for grid-connected photovoltaic systems," Sol. Energy, vol. 80, no. 12, pp. 1517-1539, 2006.

[93] D. Feldman, V. Ramasamy, R. Fu, A. Ramdas, J. Desai, and R. Margolis, "U.S. Solar Photovoltaic System and Energy Storage Cost Benchmark: Q1 2020," NREL, Golden, CO, USA, Tech. Rep. NREL/TP-6A20-77324, 2021.
[94] P. Hacke et al., "A status review of photovoltaic power conversion equipment reliability, safety, and quality assurance protocols," Renew. Sustain. Energy Rev., vol. 82, part 1, pp. 1097-1112, 2018.
[95] G. Zini, C. Mangeant, and J. Merten, "Reliability of large-scale grid-connected photovoltaic systems," Renew. Energy, vol. 36, no. 9, pp. 2334-2340, 2011.
[96] A. Golnas, "PV system reliability: An operator's perspective," IEEE J. Photovolt., vol. 3, no. 1, pp. 416-421, 2013.
[97] T. Huld and A. M. G. Amillo, "Estimating PV module performance over large geographical regions: The role of irradiance, air temperature, wind speed and solar spectrum," Energies, vol. 8, no. 6, pp. 5159-5181, 2015.
[98] A. Woyte, J. Nijs, and R. Belmans, "Partial shadowing of photovoltaic arrays with different system configurations: Literature review and field test results," Sol. Energy, vol. 74, no. 3, pp. 217-233, 2003.
[99] S. Guo, T. M. Walsh, and M. Peters, "Vertically mounted bifacial photovoltaic modules: A global analysis," Energy, vol. 61, pp. 447-454, 2013.
[100] A. Krizhevsky, I. Sutskever, and G. E. Hinton, "ImageNet classification with deep convolutional neural networks," Adv. Neural Inf. Process. Syst., vol. 25, pp. 1097-1105, 2012.
[101] F. A. Gers, J. Schmidhuber, and F. Cummins, "Learning to forget: Continual prediction with LSTM," Neural Comput., vol. 12, no. 10, pp. 2451-2471, 2000.
[102] R. S. Sutton and A. G. Barto, Reinforcement Learning: An Introduction, 2nd ed. Cambridge, MA, USA: MIT Press, 2018.
[103] M. Ribeiro, K. Grolinger, H. F. ElYamany, W. A. Higashino, and M. A. M. Capretz, "Transfer learning with seasonal and trend adjustment for cross-building energy forecasting," Energy Build., vol. 165, pp. 352-363, 2018.
[104] R. Ahmed, V. Sreeram, Y. Mishra, and M. D. Arif, "A review and evaluation of the state-of-the-art in PV solar power forecasting: Techniques and optimization," Renew. Sustain. Energy Rev., vol. 124, p. 109792, 2020.
[105] X. Tian, Y. Ma, S. Sui, J. Wang, and W. Qi, "Experimental validation of reconfiguration algorithms for partially shaded photovoltaic systems," Sol. Energy, vol. 208, pp. 234-244, 2020.
[106] G. Velasco-Quesada, F. Guinjoan-Gispert, R. Pique-Lopez, M. Roman-Lumbreras, and A. Conesa-Roca, "Electrical PV array reconfiguration strategy for energy extraction improvement in grid-connected PV systems," IEEE Trans. Ind. Electron., vol. 56, no. 11, pp. 4319-4331, 2009.
[107] C. Deline, S. MacAlpine, B. Marion, F. Toor, A. Asgharzadeh, and J. S. Stein, "Assessment of photovoltaic module-level power electronics," NREL, Golden, CO, USA, Tech. Rep. NREL/TP-5200-67453, 2017.
[108] Y. Hu, W. Cao, J. Wu, B. Ji, and D. Holliday, "Thermography-based virtual MPPT scheme for improving PV energy efficiency under partial shading conditions," IEEE Trans. Power Electron., vol. 29, no. 11, pp. 5667-5672, 2014.
[109] S. M. MacAlpine, R. W. Erickson, and M. J. Brandemuehl, "Characterization of power optimizer potential to increase energy capture in photovoltaic systems operating under nonuniform conditions," IEEE Trans. Power Electron., vol. 28, no. 6, pp. 2936-2945, 2013.
[110] V. Quaschning and R. Hanitsch, "Numerical simulation of current-voltage characteristics of photovoltaic systems with shaded solar cells," Sol. Energy, vol. 56, no. 6, pp. 513-520, 1996.
[111] N. Femia, G. Lisi, G. Petrone, G. Spagnuolo, and M. Vitelli, "Distributed maximum power point tracking of photovoltaic arrays: Novel approach and system analysis," IEEE Trans. Ind. Electron., vol. 55, no. 7, pp. 2610-2621, 2008.

[112] K. Sundareswaran, S. Peddapati, and S. Palani, "Application of random search method for maximum power point tracking in partially shaded photovoltaic systems," IET Renew. Power Gener., vol. 8, no. 6, pp. 670-678, 2014.
[113] S. A. Rizzo and G. Scelba, "ANN based MPPT method for rapidly variable shading conditions," Appl. Energy, vol. 145, pp. 124-132, 2015.
[114] K. H. Chao, P. Y. Chen, M. H. Wang, and C. T. Chen, "An intelligent maximum power point tracking method based on extension neural network for PV systems," Expert Syst. Appl., vol. 42, no. 1, pp. 751-758, 2015.
[115] A. Gupta, P. Kumar, R. K. Pachauri, and Y. K. Chauhan, "Performance analysis of neural network and fuzzy logic based MPPT techniques for solar PV systems," Arch. Electr. Eng., vol. 65, no. 4, pp. 737-751, 2016.
[116] D. Sera, L. Mathe, T. Kerekes, S. V. Spataru, and R. Teodorescu, "On the perturb-and-observe and incremental conductance MPPT methods for PV systems," IEEE J. Photovolt., vol. 3, no. 3, pp. 1070-1078, 2013.
[117] M. Seyedmahmoudian et al., "Simulation and hardware implementation of new maximum power point tracking technique for partially shaded PV system using hybrid DEPSO method," IEEE Trans. Sustain. Energy, vol. 6, no. 3, pp. 850-862, 2015.
[118] B. Kroposki et al., "Achieving a 100% renewable grid: Operating electric power systems with extremely high levels of variable renewable energy," IEEE Power Energy Mag., vol. 15, no. 2, pp. 61-73, 2017.
[119] J. P. Storey, P. R. Wilson, and D. Bagnall, "Improved optimization strategy for irradiance equalization in dynamic photovoltaic arrays," IEEE Trans. Power Electron., vol. 28, no. 6, pp. 2946-2956, 2013.
[120] B. Patnaik, J. D. Sharma, K. Kanungo, and C. P. Nayak, "Experimental validation of a novel reconfiguration algorithm for solar PV arrays subject to uniform and non-uniform irradiance," IET Renew. Power Gener., vol. 13, no. 9, pp. 1602-1612, 2019.
[121] P. L. Carotenuto, P. Manganiello, G. Petrone, and G. Spagnuolo, "Online recording a PV module fingerprint," IEEE J. Photovolt., vol. 4, no. 2, pp. 659-668, 2014.
[122] L. F. L. Villa, D. Picault, B. Raison, S. Bacha, and A. Labonne, "Maximizing the power output of partially shaded photovoltaic plants through optimization of the interconnections among its modules," IEEE J. Photovolt., vol. 2, no. 2, pp. 154-163, 2012.
[123] Y. Wang, Y. Lin, T. Tang, and S. Wang, "Optimization of PV array configurations under dynamic shading conditions," IEEE 43rd Photovolt. Spec. Conf., pp. 2256-2261, 2016.
[124] A. Kouchaki, H. Iman-Eini, and B. Asaei, "A new maximum power point tracking strategy for PV arrays under uniform and non-uniform insolation conditions," Sol. Energy, vol. 91, pp. 221-232, 2013.
[125] P. Romano, R. Candela, M. Cardinale, V. Li Vigni, D. Musso, and E. Riva Sanseverino, "Optimization of photovoltaic energy production through an efficient switching matrix," J. Sustain. Dev. Energy, Water Environ. Syst., vol. 1, no. 3, pp. 227-236, 2013.
[126] M. Z. S. El-Dein, M. Kazerani, and M. M. A. Salama, "An optimal total cross tied interconnection for reducing mismatch losses in photovoltaic arrays," IEEE Trans. Sustain. Energy, vol. 4, no. 1, pp. 99-107, 2013.
[127] S. Pareek and R. Dahiya, "Enhanced power generation of partial shaded photovoltaic fields by forecasting the interconnection of modules," Energy, vol. 95, pp. 561-572, 2016.
[128] J. Camarillo-Peñaranda, D. González-Montoya, and C. Duarte, "Real-time forecast MPPT for PV systems under rapidly changing irradiance events," IEEE 46th Photovolt. Spec. Conf., pp. 1602-1607, 2019.

[129] P. M. Rodrigo, E. F. Fernández, F. M. Almonacid, and P. J. Pérez-Higueras, "A simple accurate model for the calculation of shading power losses in photovoltaic generators," Sol. Energy, vol. 93, pp. 322-333, 2013.
[130] A. Ibrahim and A. Abusorrah, "The impact of cloud edge effect on the PV output power," IEEE Sustainable Energy Technologies Conf., pp. 1-5, 2019.
[131] O. Comstock, "Economic analysis of field-level reconfiguration for crystalline silicon PV arrays," IEEE 44th Photovolt. Spec. Conf., pp. 2349-2354, 2017.
[132] Electricity Advisory Committee, "Consumer Acceptance of New Electricity Technologies," U.S. Department of Energy, Washington DC, USA, 2020.
[133] E. Vartiainen, G. Masson, C. Breyer, D. Moser, and E. Román Medina, "Impact of weighted average cost of capital, capital expenditure, and other parameters on future utility-scale PV levelised cost of electricity," Prog. Photovolt. Res. Appl., vol. 28, no. 6, pp. 439-453, 2020.
[134] D. Feldman, M. Zwerling, and R. Margolis, "Q2/Q3 2022 Solar Industry Update," NREL, Golden, CO, USA, Tech. Rep. NREL/PR-7A40-84149, 2022.
[135] T. Doyle, P. Kokolis, and T. Erion-Lorico, "PV Module Durability Scorecard," PVEL LLC, Berkeley, CA, USA, 2022.
[136] P. Singh, S. Lal, and M. Husain, "Reliability analysis of series-parallel solar photovoltaic system considering the effect of partial shading," J. Building Eng., vol. 33, p. 101613, 2021.
[137] SolarPower Europe, "Operation & Maintenance Best Practice Guidelines Version 5.0," SolarPower Europe, Brussels, Belgium, 2021.
[138] E. Collins, M. Dvorack, J. Mahn, M. Mundt, and M. Quintana, "Reliability and availability analysis of a fielded photovoltaic system," IEEE 34th Photovolt. Spec. Conf., pp. 2316-2321, 2009.
[139] D. Picault, B. Raison, S. Bacha, J. de la Casa, and J. Aguilera, "Forecasting photovoltaic array power production subject to mismatch losses," Sol. Energy, vol. 84, no. 7, pp. 1301-1309, 2010.
[140] International Renewable Energy Agency (IRENA), "End-of-Life Management: Solar Photovoltaic Panels," IRENA, Abu Dhabi, 2016.
[141] X. Nguyen, D. Nguyen, D. Lu, S. Kamalasadan, and M. Farhadi, "Robust Deep Learning-Based Detection and Diagnosis of Faults in Photovoltaic Arrays," IEEE Trans. Power Electronics, vol. 36, no. 10, pp. 11187-11202, 2021.
[142] A. Dolara, F. Grimaccia, S. Leva, M. Mussetta, and E. Ogliari, "A physical hybrid artificial neural network for short term forecasting of PV plant power output," Energies, vol. 8, no. 2, pp. 1138-1153, 2015.
[143] M. Cao, P. V. Chao, L. Yang, F. Wang, and Y. Xu, "Deep reinforcement learning based energy management of hybrid battery-supercapacitor system in a microgrid," IEEE Energy Convers. Congr. Expo., pp. 902-908, 2020.
[144] W. Zhang, W. Wu, X. Ma, F. Yang, and Y. Jin, "A deep learning approach for fault diagnosis of photovoltaic arrays based on electrical measurements," IEEE Sustainable Power Energy Conf., pp. 2520-2526, 2019.
[145] V. Mishra, P. Singh, and K. Vasudevan, "Detection and classification of faults in photovoltaic arrays using machine learning techniques," IEEE 46th Photovolt. Spec. Conf., pp. 1602-1607, 2019.
[146] B. Palmintier et al., "On the path to SunShot: Emerging issues and challenges in integrating solar with the distribution system," NREL, Golden, CO, USA, Tech. Rep. NREL/TP-5D00-65331, 2016.
[147] M. Lave, J. Kleissl, and J. S. Stein, "A wavelet-based variability model (WVM) for solar PV power plants," IEEE Trans. Sustain. Energy, vol. 4, no. 2, pp. 501-509, 2013.
[148] J. von Appen, T. Stetz, M. Braun, and A. Schmiegel, "Local voltage control strategies for PV storage systems in distribution grids," IEEE Trans. Smart Grid, vol. 5, no. 2, pp. 1002-1009, 2014.

[149] R. Hanna, J. Kleissl, A. Nottrott, and M. Ferry, "Energy dispatch schedule optimization for demand charge reduction using a photovoltaic-battery storage system with solar forecasting," Sol. Energy, vol. 103, pp. 269-287, 2014.
[150] D. C. Jordan, S. R. Kurtz, K. VanSant, and J. Newmiller, "Compendium of photovoltaic degradation rates," Prog. Photovolt. Res. Appl., vol. 24, no. 7, pp. 978-989, 2016.
[151] T. Huld, G. Friesen, A. Skoczek, R. P. Kenny, T. Sample, M. Field, and E. D. Dunlop, "A power-rating model for crystalline silicon PV modules," Sol. Energy Mater. Sol. Cells, vol. 95, no. 12, pp. 3359-3369, 2011.
[152] D. Feldman, K. Horowitz, B. Palmintier, R. Fu, and R. Margolis, "Quantifying innovation in the U.S. solar industry: An exploratory statistical analysis," NREL, Golden, CO, USA, Tech. Rep. NREL/TP-6A20-77961, 2021.
[153] C. E. Valdivia et al., "Bifacial photovoltaic module energy yield: A review of field data, prediction tools, and cost implications," Prog. Photovolt. Res. Appl., vol. 29, no. 12, pp. 1331-1357, 2021.
[154] A. Sangwongwanich, Y. Yang, and F. Blaabjerg, "A cost-effective power ramp-rate control strategy for single-phase two-stage grid-connected photovoltaic systems," IEEE Trans. Energy Convers., vol. 32, no. 3, pp. 1151-1162, 2017.
[155] Y. Levron, D. R. Clement, B. Choi, C. Olalla, and D. Maksimovic, "Control of submodule integrated converters in the isolated-port differential power-processing photovoltaic architecture," IEEE J. Emerg. Sel. Top. Power Electron., vol. 2, no. 4, pp. 821-832, 2014.
[156] X. Li et al., "Recent advances in wide-bandgap semiconductor power devices for high-frequency applications," Eng. Sci., vol. 16, pp. 165-185, 2021.
[157] K. W. Kow, Y. W. Wong, R. K. Rajkumar, and R. K. Rajkumar, "A review on performance of artificial intelligence and conventional method in mitigating PV grid-tied related power quality events," Renew. Sustain. Energy Rev., vol. 56, pp. 334-346, 2016.
[158] C. P. Cameron, W. E. Boyson, and D. M. Riley, "Comparison of PV system performance-model predictions with measured PV system performance," IEEE 34th Photovolt. Spec. Conf., pp. 1-6, 2008.
[159] N. Martin-Chivelet and D. Montero-Gomez, "Optimizing photovoltaic self-consumption in office buildings," Energy Build., vol. 150, pp. 71-80, 2017.
[160] C. Deline et al., "A simplified model of uniform shading in large photovoltaic arrays," Sol. Energy, vol. 96, pp. 274-282, 2013.
[161] K. Ding, X. Bian, H. Liu, and T. Peng, "A MATLAB-Simulink-based PV module model and its application under conditions of nonuniform irradiance," IEEE Trans. Energy Convers., vol. 27, no. 4, pp. 864-872, 2012.
[162] SolarEdge Technologies Inc., "Global Trends in C&I Solar," SolarEdge White Paper, Herzliya, Israel, 2021.